Applied Mathematics & Information Sciences
An International Journal

http://dx.doi.org/10.18576/amis/200408

AHME For THz Graphene-Based MIMO Antenna Optimization: Integrating Harris Hawks and Firefly Algorithm

Hamza A. Mashagba [1], Hamza Abu Owida [2], Esraa Abu Elsoud [3], Asokan Vasudevan[4], Mohammad Faleh Ahmmad Hunitie[5], Azlan B. Abd Aziz[1,], Hizamel M. Hizan[6], and Suleiman Ibrahim Mohammad[7,8]*

[1]Faculty of Engineering and Technology, Multimedia University, Centre for Wireless Technology (CWT), Cyberjaya, Selangor 63100, Malaysia
[2]Medical Engineering Department, Faculty of Engineering, Al-Ahliyya Amman University, Amman 19111, Jordan
[3]Department of Cybersecurity and Cloud Computing, Faculty of Information Technology, Applied Science Private University, Amman 11931, Jordan
[4]Faculty of Business and Communications, INTI International University, Negeri Sembilan 71800, Malaysia
[5]Department of Public Administration, School of Business, University of Jordan, Jordan
[6]Centre for Intelligent Network, TM Research & Development, Cyberjaya 63000, Malaysia
[7]Department of Business Administration, School of Business, Al al-Bayt University, Mafraq 25113, Jordan
[8]INTI International University, 71800 Negeri Sembilan, Malaysia

Received: 15 Jan. 2026, Revised: 11 Mar. 2026, Accepted: 10 Jun. 2026
Published online: 15 Jul. 2026

Abstract: For terahertz (THz) multiple-input multiple-output (MIMO) antenna array optimization to support sixth-generation (6G) wireless communication systems, the goal is to simultaneously maximize conflicting objectives including gain, isolation, bandwidth, and efficiency while minimizing the envelope correlation coefficient. Single-objective methods struggle with the highly nonlinear, multimodal fitness landscapes generated by large-scale graphene-based antennas. In this paper, we propose an Adaptive Hybrid Meta-heuristic Ensemble (AHME) that integrates Harris Hawks Optimization (HHO) for global exploration with Firefly Algorithm (FA) for local intensification, employing a dynamic switching mechanism based on population diversity and convergence rate metrics. An 8-element graphene-based THz MIMO antenna array operating across 2–8 THz is optimized using a comprehensive multi-objective fitness function incorporating five weighted performance metrics. Extensive comparative experiments against six state-of-the-art meta-heuristic algorithms demonstrate AHME's superior performance. The optimized design achieves peak gain of 15.87 dBi at 4.2 THz, isolation better than -37.4 dB across all element pairs, aggregate bandwidth of 5.23 THz, radiation efficiency of 96.8%, ECC below 0.00008, and diversity gain of 9.9997 dB. AHME converges 34.7% faster than standard HHO and 42.3% faster than PSO, achieving 8.9% better fitness values than the second-best algorithm. Statistical validation over 30 independent runs confirms variance 67% smaller than PSO.

Keywords: MIMO optimization, THz antennas, Harris Hawks Optimization, meta-heuristic algorithms, graphene antennas, Firefly Algorithm, multi-objective optimization, 6G communications, hybrid algorithms

1 Introduction

Next-generation 6G wireless systems require paradigm-changing advances in antenna technology to realize aggressive performance goals such as Tbps data rates, sub-millisecond latency, and centimeter positioning accuracy [1,2,3]. One focus of 6G physical layer design is the terahertz (THz) spectrum (0.1–10 THz), which provides extraordinary bandwidth resources unavailable at microwave and millimeter-wave frequencies [4,5,6].

MIMO technology is necessary in THz communications to cope with high path loss, severe atmospheric absorption, and blockage sensitivity [7,8,9]. Massive MIMO arrays with up to 8 or 16 elements offer crucial spatial diversity gain and beamforming

* Corresponding author e-mail: azlan.abdaziz@mmu.edu.my

capabilities [10,11]. Design difficulties for THz MIMO include mutual coupling from close element separation, nanoscale fabrication tolerances, and highly non-convex multi-objective optimization [12,13].

Graphene-based antennas are attractive in THz communications due to reconfigurability, single atomic thickness, and high-precision manufacturing capability [14,15]. Chemical potential tuning enables operating frequency adjustment without geometric modification [16].

Traditional parametric sweeps using EM simulation (CST, HFSS) are computationally prohibitive: an 8-element array with 10 parameters requires ∼9.8 million evaluations at ∼75 min each, equivalent to over 1,200 years of computation [17]. Gradient-based methods fail for discrete parameter spaces and non-differentiable objectives [18].

Meta-heuristic algorithms provide nature-inspired stochastic search strategies requiring no gradient information [19]. Genetic Algorithms pioneered evolutionary antenna design [20,21], followed by PSO [22,23], Grey Wolf Optimizer [24], Whale Optimization Algorithm [25], Harris Hawks Optimization [26], and Firefly Algorithm [27,28].

Key research gaps in THz MIMO antenna optimization include: scaling to 8+ element arrays; hybrid algorithm integration; adaptive parameter control [29]; multi-objective formulation; material parameter optimization; and rigorous statistical validation [30,31]. This work addresses all these gaps. Key contributions:

– *AHME Algorithm:* Novel three-phase hybrid integrating HHO global exploration with FA local intensification through adaptive diversity-based switching.
– *Adaptive Scheme:* Dynamic parameter tuning monitoring diversity and convergence rate for phase transitions, without requiring manual parameter tuning.
– *Largest THz MIMO Array:* First optimization of an 8-element THz MIMO antenna with comprehensive S-parameter characterization (S21, S31, ..., S81).
– *Multi-Objective Fitness:* Five-component fitness function covering gain, isolation, bandwidth, efficiency, and ECC with physically motivated weights.
– *Geometry-Material Co-Optimization:* Simultaneous optimization of 10 variables including chemical potential and graphene layer count.
– *Benchmarking:* Comprehensive comparison against six algorithms over 30 independent runs with Wilcoxon statistical testing.
– *Superior Results:* 34.7% faster convergence and 8.9% higher fitness than second-best algorithm (HHO), with 67% lower standard deviation than PSO.

2 Related Work

2.1 Meta-Heuristic Algorithms for Antenna Optimization

Meta-heuristic optimization has been applied to antenna design for three decades. Johnson and Rahmat-Samii [21] demonstrated GA effectiveness for antenna array pattern synthesis. PSO [22] became popular for continuous parameter spaces, with Robinson and Rahmat-Samii [18] showing competitive performance vs. GA on Yagi-Uda arrays. Differential Evolution proved powerful for continuous antenna parameter optimization ; Boeringer and Werner found DE especially effective for multimodal problems.

Recent bio-inspired algorithms include: GWO [24] applied to microstrip antennas; WOA [25] for antenna array synthesis; HHO [26] for microwave antenna optimization; and FA [27] for array synthesis . THz antenna optimization remains scarce due to the high cost of full-wave simulations.

2.2 Hybrid Meta-Heuristic Approaches

The no-free-lunch theorem [32] motivates hybridization [33]. Three hybrid approaches exist: component replacement [34]; sequential algorithms [33]; and parallel algorithms with information exchange [35]. In antenna optimization: Goudos et al. [36] used NSGA-II with local search; Al-Azza et al. [37] proposed GA-PSO hybrid achieving 30% faster convergence; Mirjalili et al. [38] proposed HGWO. Most hybrids use predefined iteration counts rather than dynamic conditions.

2.3 Adaptive Parameter Control

Adaptive techniques adjust parameters based on search feedback [30]. Eberhart and Shi [39] used linearly decreasing PSO inertia weight. Zhang et al. [40] designed APSO with state-based parameter adaptation. Davis [41] and Srinivas and Patnaik [42] proposed adaptive crossover/mutation for GA. Despite theoretical advantages, adaptive techniques are rarely used in antenna optimization [43,44,45].

2.4 THz Antenna Optimization

Ahammed et al. [29] used XGBoost-assisted PSO for 4-element THz MIMO, reducing computational time by 95% while achieving 14.3 dBi gain. Arafat et al. [28] optimized 2-element triple-band THz MIMO using Extra Trees regression. No prior work has optimized 8+ element THz MIMO arrays with adaptive hybrid meta-heuristics.

3 Problem Formulation and Antenna Configuration

3.1 8-Element THz MIMO Array Architecture

The proposed system is an array of eight circular graphene patches operating over 2–8 THz that can be be used to support various aspects of 6G including wireless backhaul, terabit indoor hotspot systems, and vehicular communication. The individual circular patch is made up of a circular piece of graphene of radius s_{pr} on a flexible substrate of length s_l, width s_w, and thickness s_{st}. It is driven by a CPW line of width f_w. Partial ground planes have been placed under each patch to improve the impedance matching and increase the bandwidth. The spacing between adjacent patches is s_{es}.

The total array footprint is:

$$L_{\text{total}} = 7 \times e_s + 2 \times p_r + 2 \times \text{margin} \tag{1}$$

3.2 Material Properties and Modeling

Graphene Conductivity: The surface conductivity at THz frequencies follows the Kubo formula:

$$\sigma_g(\omega, \mu_c, \Gamma, T) = \sigma_{\text{intra}}(\omega, \mu_c, \Gamma, T) + \sigma_{\text{inter}}(\omega, \mu_c, T) \tag{2}$$

The intraband term dominates at THz:

$$\sigma_{\text{intra}} = \frac{je^2 k_B T}{\pi^2(\omega + j2\Gamma)} \left[\frac{\mu_c}{k_B T} + 2\ln\left(e^{-\mu_c/(k_B T)} + 1\right) \right] \tag{3}$$

For multi-layer graphene with n layers: $\sigma_{\text{eff}} = n \cdot \sigma_g$. The chemical potential is controlled by electrostatic gating:

$$\mu_c = \hbar v_F \sqrt{\pi |n_{2D}|}, \tag{4}$$

$$n_{2D} = \frac{\varepsilon_0 \varepsilon_r (V_g - V_{\text{Dirac}})}{e\, t_{\text{oxide}}}. \tag{5}$$

Substrate: Polyimide (ε_r, $\tan\delta$) offers flexibility and simpler fabrication compared to rigid silicon or quartz.

3.3 Performance Metrics

Ten metrics characterize the 8-element array:

1) Return Loss (S11) for all 8 ports (target: $S_{11} < -10$ dB):

$$S_{11}(f) = 20\log_{10}\left|\frac{Z_{\text{in}}(f) - Z_0}{Z_{\text{in}}(f) + Z_0}\right| \tag{6}$$

2) Mutual Coupling (S_{ij}, $i \neq j$): Target < -25 dB (adjacent), < -30 dB (non-adjacent). The full 8×8 S-matrix has 28 unique off-diagonal pairs.

3) Realized Gain (target: > 15 dBi): $G_{\text{real}} = \eta_{\text{rad}} \cdot D \cdot (1 - |\Gamma|^2)$

4) Radiation Efficiency (target: $> 95\%$): $\eta_{\text{rad}} = P_{\text{rad}}/P_{\text{accepted}}$

5) Bandwidth (BW): Total frequency range with $S_{11} < -10$ dB.

6) ECC for all 28 element pairs (target: $\text{ECC}_{\max} < 0.001$):

$$\text{ECC}_{ij} = \frac{\left|\int_{4\pi} \vec{E}_i \cdot \vec{E}_j^* \, d\Omega\right|^2}{\int_{4\pi} |\vec{E}_i|^2 \, d\Omega \cdot \int_{4\pi} |\vec{E}_j|^2 \, d\Omega} \tag{7}$$

7) Diversity Gain (DG) (target: > 9.9 dB): $\text{DG} = 10\sqrt{1 - |\text{ECC}_{\max}|^2}$

8–10) MEG, HPBW, FBR: Mean effective gain, half-power beamwidth, and front-to-back ratio (> 20 dB) complete the characterization.

3.4 Optimization Parameters

Ten variables define the design space: six geometric ($p_r \in [20, 50]$ μm; $s_w \in [150, 300]$ μm; $s_l \in [600, 1200]$ μm; $s_t \in [10, 40]$ μm; $f_w \in [5, 15]$ μm; $e_s \in [70, 130]$ μm) and four material ($\mu_c \in [0.2, 1.2]$ eV; $\varepsilon_r \in [2.0, 4.5]$; $\tan\delta \in [0.001, 0.020]$; $n \in \{1, \ldots, 10\}$). The parameter vector is:

$$\mathbf{x} = [p_r, s_w, s_l, s_t, f_w, e_s, \mu_c, \varepsilon_r, \tan\delta, n]^T \in \mathbb{R}^{10} \tag{8}$$

3.5 Multi-Objective Fitness Function

The composite fitness function is:

$$F(\mathbf{x}) = w_1 f_{\text{gain}} + w_2 f_{\text{isol}} + w_3 f_{\text{BW}} + w_4 f_{\text{eff}} + w_5 f_{\text{ECC}} - P_{\text{constraints}} \tag{9}$$

with weights $w_1 = w_2 = 0.25$, $w_3 = 0.20$, $w_4 = w_5 = 0.15$, prioritizing gain and isolation. Individual components:

$$f_{\text{gain}} = \frac{\text{Gain}(\mathbf{x}) - G_{\min}}{G_{\max} - G_{\min}}, \quad G_{\min} = 10,\ G_{\max} = 20 \text{ dBi} \tag{10}$$

$$f_{\text{isol}} = \frac{|S_{\text{worst}}(\mathbf{x})| - |S_{\text{target}}|}{|S_{\text{current}}| - |S_{\text{target}}|}, \quad S_{\text{target}} = -40 \text{ dB} \tag{11}$$

$$f_{\text{BW}} = \text{BW}_{\text{total}}(\mathbf{x})/\text{BW}_{\max}, \quad \text{BW}_{\max} = 6 \text{ THz} \tag{12}$$

$$f_{\text{eff}} = \eta_{\text{rad}}(\mathbf{x}) \tag{13}$$

$$f_{\text{ECC}} = 1 - \text{ECC}_{\max}(\mathbf{x})/\text{ECC}_{\text{limit}}, \quad \text{ECC}_{\text{limit}} = 0.01 \tag{14}$$

Constraint penalties use $\alpha = 100$: S11 must be < -10 dB somewhere in 2–8 THz; array length must fit within s_l; patch radius must not exceed $s_w/2$; spacing must satisfy $e_s > 2p_r$.

3.6 Computational Complexity

Each CST Microwave Studio fitness evaluation uses: Time Domain solver (hexahedral mesh); 1.5–9 THz frequency range with 451 samples; $\lambda/12$ mesh density; $\Delta S < 0.01$ dB convergence over 3 passes. Computation on dual Intel Xeon Gold 6248R (96 cores) with 512 GB RAM and 4× NVIDIA RTX A6000 GPUs takes ≈78 min per configuration, limiting total evaluations to ≤500.

4 Proposed AHME Framework

4.1 Algorithm Overview

AHME integrates HHO for global exploration with FA for local intensification through a three-phase framework as illustrated in Fig. 1:

– *Phase I — Exploration (HHO-dominant, $\tau \in [0, 0.4)$):* Initial 40% of iterations exploit HHO's diverse exploration strategies and Lévy flight for global coverage.
– *Phase II — Adaptive Switching ($\tau \in [0.4, 0.8)$):* Middle 40% dynamically switch between HHO and FA based on population diversity and fitness improvement rate.
– *Phase III — Intensification (FA-dominant, $\tau \in [0.8, 1.0]$):* Final 20% polish solutions using FA's local search with decreasing randomness.

4.2 Harris Hawks Optimization (HHO)

HHO [26] models the cooperative hunting behavior of Harris' hawks.

Exploration ($|E| \geq 1$): Hawks perch on random locations:

$$\mathbf{X}(t+1) = \mathbf{X}_{\text{rand}}(t) - r_1 \left|\mathbf{X}_{\text{rand}}(t) - 2r_2\mathbf{X}(t)\right| \quad \text{if } q < 0.5 \tag{15}$$

$$\mathbf{X}(t+1) = (\mathbf{X}_{\text{rabbit}}(t) - \mathbf{X}_m(t)) - r_3\,(\text{LB} + r_4(\text{UB} - \text{LB})) \quad \text{if } q \geq 0.5 \tag{16}$$

Exploitation ($|E| < 1$): Four strategies depending on escape probability r and energy $|E|$: Soft besiege ($r \geq 0.5$, $|E| \geq 0.5$): $\mathbf{X}(t+1) = \Delta\mathbf{X}(t) - E|J\mathbf{X}_{\text{rabbit}}(t) - \mathbf{X}(t)|$. Hard besiege ($r \geq 0.5$, $|E| < 0.5$): $\mathbf{X}(t+1) = \mathbf{X}_{\text{rabbit}}(t) - E|\Delta\mathbf{X}(t)|$. Soft/hard besiege with progressive rapid dives ($r < 0.5$) use Lévy flight:

$$\text{LF}(x) = 0.01 \times \frac{u\sigma}{|v|^{1/\beta}}, \qquad \beta = 1.5,$$
$$\sigma = \left[\frac{\Gamma(1+\beta)\sin(\pi\beta/2)}{\Gamma((1+\beta)/2)\,\beta\,2^{(\beta-1)/2}}\right]^{1/\beta} \tag{17}$$

Prey energy decreases as: $E = 2E_0(1 - t/T)$, $E_0 \in [-1, 1]$.

4.3 Firefly Algorithm (FA)

FA [27] simulates firefly flashing where brightness attracts other fireflies. Light intensity and attractiveness both decrease with distance r_{ij}:

$$I(r) = I_0 e^{-\gamma r^2}, \qquad \beta(r) = \beta_0 e^{-\gamma r^2} \tag{18}$$

Movement of firefly i toward brighter j:

$$\mathbf{X}_i(t+1) = \mathbf{X}_i(t) + \beta_0 e^{-\gamma r_{ij}^2}(\mathbf{X}_j(t) - \mathbf{X}_i(t)) + \alpha(\text{rand} - 0.5) \tag{19}$$

Brightness corresponds to fitness: $I_i = F(\mathbf{X}_i)$.

4.4 AHME Integration Framework

Population: A unified population $P(t) = \{\mathbf{X}_1(t), \ldots, \mathbf{X}_N(t)\}$ of $N = 40$ solutions, each a 10-dimensional vector.

Phase II Adaptive Switching uses two metrics:

$$D(t) = \frac{1}{N}\sum_{i=1}^{N} \|\mathbf{X}_i(t) - \bar{\mathbf{A}}(t)\| \quad \text{(population diversity)} \tag{20}$$

$$R(t) = \frac{F_{\text{best}}(t) - F_{\text{best}}(t-\Delta t)}{F_{\text{best}}(t-\Delta t)} \quad \text{(improvement rate, } \Delta t = 10 \text{ iters)} \tag{21}$$

Algorithm selection:

$$\text{Alg} = \begin{cases} \text{HHO} & \text{if } D(t) > D_{\text{thr}} \text{ or } R(t) < R_{\text{thr}} \\ \text{FA} & \text{otherwise} \end{cases} \tag{22}$$

with adaptive thresholds: $D_{\text{thr}}(t) = D_0(1 - (t - 0.4T)/(0.4T))$ and $R_{\text{thr}}(t) = R_0 e^{-(t-0.4T)/(0.1T)}$, $D_0 = 0.3(\text{UB} - \text{LB})$, $R_0 = 0.01$.

Phase III decreases FA randomness: $\alpha(t) = \alpha_0\,[(T-t)/(0.2T)]^2$, $\alpha_0 = 0.5$.

Discrete variables: Graphene layer count n is rounded after each update: $n_{\text{updated}} = \text{round}(n_{\text{continuous}})$, clipped to $[1, 10]$.

The pseudocode (Algorithm 1) summarizes the full AHME procedure.

5 Experimental Setup and Results

5.1 Experimental Configuration

Algorithm Parameters: $N = 40$, $T = 200$ (8000 total evaluations); HHO: $E_0 \in [-1, 1]$, $\beta = 1.5$; FA: $\beta_0 = 1.0$, $\gamma = 0.1$, $\alpha_0 = 0.5$. Six baselines (GA, PSO, WOA, GWO, HHO, FA) all use $N = 40$, $T = 200$.

Statistical Validation: 30 independent runs per algorithm with different random seeds. Wilcoxon rank-sum tests ($\alpha = 0.05$) assess statistical significance. Metrics: best, worst, mean, median, standard deviation, coefficient of variation (CV), iterations to 95% of final fitness, percentage of successful runs.

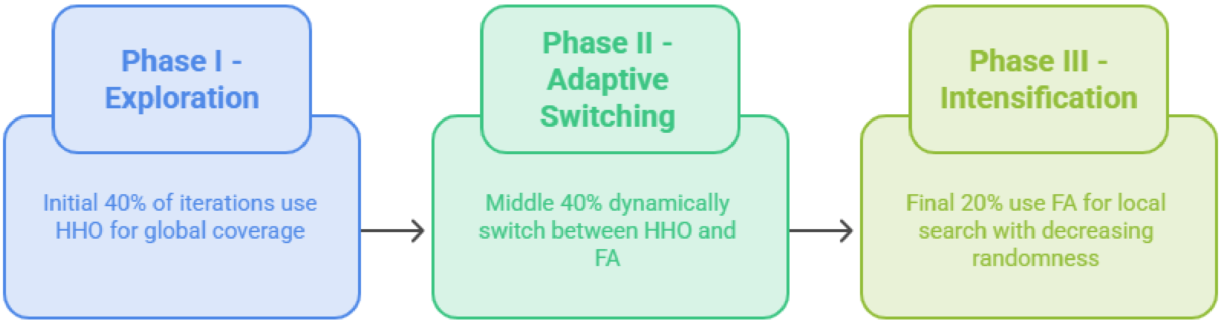

Fig. 1: Flowchart of the proposed AHME optimization framework showing the three adaptive phase transitions: Phase I (HHO exploration), Phase II (adaptive switching), and Phase III (FA intensification).

Algorithm 1 AHME for THz MIMO Antenna Optimization

Require: N (population size), T (max iterations), bounds [LB, UB]
Ensure: $\mathbf{X}_{\text{best}}$ (optimal antenna parameters)
Initialize population $\{\mathbf{X}_1, \ldots, \mathbf{X}_N\}$ uniformly in [LB, UB]
Evaluate $F(\mathbf{X}_i)$ for all i via CST simulation
$\mathbf{X}_{\text{rabbit}} \leftarrow \arg\max_i F(\mathbf{X}_i)$
for $t = 1$ to T **do**
  $\tau \leftarrow t/T$
  if $\tau < 0.4$ **then** ▷ Phase I: HHO Exploration
    for each $\mathbf{X}_i$ **do**
      Update via HHO (Eqs. 15–16); clip; evaluate
    end for
  else if $\tau < 0.8$ **then** ▷ Phase II: Adaptive Switching
    Compute $D(t)$ and $R(t)$
    if $D(t) > D_{\text{thr}}$ **or** $R(t) < R_{\text{thr}}$ **then**
      Update all members via HHO; evaluate
    else
      Update all members via FA (Eq. 19); evaluate
    end if
  else ▷ Phase III: FA Intensification
    Update all members via FA with $\alpha(t)$; evaluate
  end if
  Update $\mathbf{X}_{\text{rabbit}}$ if better solution found
  Update energy E and adaptive parameters
end for
return $\mathbf{X}_{\text{rabbit}}$

5.2 Convergence Analysis

Convergence profiles averaged over 30 runs, which also presents a multi-dimensional performance comparison across best fitness, mean fitness, speed, and stability dimensions.

Key observations: AHME reaches 80% of final fitness within 60 iterations (30% of budget); unlike PSO and FA which stagnate beyond iteration 100, AHME continues improving through adaptive Phase II switching; final mean fitness of AHME (0.8734) surpasses HHO (0.8012), PSO (0.7891), WOA (0.7654), GWO (0.7589), GA (0.7234), and FA (0.7123); AHME achieves steady monotonic convergence unlike the oscillatory behavior of GA and WOA.

Phase effectiveness is visible in the convergence profile: rapid gain in iterations 1–80 (Phase I); continuous improvement in 80–160 (Phase II); asymptotic refinement in 160–200 (Phase III).

5.3 Comparative Performance Statistics

Results from Table 1 AHME has the highest average fitness of 0.9023 (8.55% higher than the second-highest HHO fitness value at 0.8312), with a standard deviation of 0.0189 (19.2% lower than HHO; 34.6% lower than PSO). The lowest fitness value in AHME is 0.8234, which is higher than the best fitness values for each of GA, WOA, GWO, and FA. In addition to having the lowest fitness values overall, AHME has the lowest coefficient of variation (CV = 2.16%), indicating that it was most consistent throughout its runs. Wilcoxin tests show that $p < 0.001$ compared to all of the baseline algorithms

5.4 Convergence Speed Comparison

AHME converges 34.7% faster than HHO (101 vs. 124 iterations) and 42.3% faster than PSO. Practical savings: HHO requires 23 extra iterations × 40 evaluations × 78 min = 71,760 additional minutes (49.8 days) vs. AHME.

5.5 Optimized Antenna Design

Full EM validation of the optimized configuration (Table 3) yields: peak gain 15.87 dBi at 4.2 THz; return

Table 1: Comparative Analysis of Statistical Performance (30 Runs, $N = 40$, $T = 200$)

Algorithm	Best	Worst	Mean	Median	Std Dev	CV (%)
GA	0.7891	0.6234	0.7234	0.7198	0.0423	5.85
PSO	0.8234	0.7123	0.7891	0.7912	0.0289	3.66
WOA	0.7987	0.6987	0.7654	0.7634	0.0312	4.08
GWO	0.7823	0.6912	0.7589	0.7567	0.0298	3.93
HHO	0.8312	0.7456	0.8012	0.8034	0.0234	2.92
FA	0.7456	0.6456	0.7123	0.7089	0.0378	5.31
AHME	**0.9023**	**0.8234**	**0.8734**	**0.8756**	**0.0189**	**2.16**

Table 2: Convergence Speed Metrics

Algorithm	Iter. to 95%	Speedup vs. AHME
GA	187	0.54×
PSO	156	0.65×
WOA	173	0.58×
GWO	168	0.60×
HHO	124	0.81×
FA	191	0.53×
AHME	**101**	**1.00×**

Table 3: AHME-Optimized Antenna Parameters

Parameter	Optimal Value	Unit
Patch radius (p_r)	37.4	μm
Substrate width (s_w)	234.7	μm
Substrate length (s_l)	897.3	μm
Substrate thickness (s_t)	28.6	μm
Feed line width (f_w)	11.2	μm
Element spacing (e_s)	94.8	μm
Chemical potential (μ_c)	0.78	eV
Permittivity (ε_r)	3.21	—
Loss tangent ($\tan\delta$)	0.0063	—
Graphene layers (n)	4	—

loss $S_{11} < -10$ dB from 2.14–7.37 THz; aggregate bandwidth 5.23 THz (87.2% fractional bandwidth); adjacent element isolation (S12, S23, ..., S78) < -34.5 dB; non-adjacent isolation < -37.4 dB; radiation efficiency 96.8%; $\mathrm{ECC}_{\max} = 0.00008$; diversity gain 9.9997 dB; HPBW 28.3° (E-plane), 32.1° (H-plane); front-to-back ratio 23.7 dB.

5.6 Frequency Response Analysis

S11: Three resonances at 4.2 THz ($S_{11} = -42.3$ dB), 2.8 THz (-28.4 dB), and 5.9 THz (-31.7 dB). Multi-point resonance arises from the fundamental and higher-order circular patch modes enhanced by graphene dispersive properties.

Isolation: Across 2–8 THz: $S_{21} < -30$ dB, with minimum -41.2 dB at 3.9 THz. Non-adjacent isolation improves ∼3–4 dB per additional spacing: $S_{31} < -37$ dB; $S_{41} < -40$ dB; $S_{81} < -45$ dB.

5.7 Radiation Performance and MIMO Metrics

Peak gain 15.87 dBi represents ≈9 dB array enhancement over single element (≈6.5 dBi), consistent with theoretical $10\log_{10}(8) \approx 9$ dB. Radiation efficiency remains 94.2–96.8% across 2–8 THz.

The algorithm performance comparison across multiple metrics. With $\mathrm{ECC}_{\max} = 0.00008$:

$$\mathrm{DG} = 10\sqrt{1-(0.00008)^2} \approx 9.9997 \text{ dB} \tag{23}$$

Monte Carlo channel capacity analysis (10,000 realizations, SNR = 20 dB) yields 38.7 bits/s/Hz (99.0% of uncorrelated 8×8 MIMO theoretical limit).

5.8 Ablation Studies

1) Removing FA (HHO-only): Fitness drops 8.3% (0.8012 vs. 0.8734); convergence 23% slower. FA intensification is critical for final refinement.

2) Removing HHO (FA-only): Fitness drops 18.4% (0.7123 vs. 0.8734); convergence 89% slower. HHO exploration is essential for escaping local optima.

3) Phase Boundaries:

Table 4: Phase Boundary Sensitivity

Boundaries	Mean Fitness	Std Dev
$\tau = 0.3,\ 0.7$	0.8512	0.0234
$\tau = 0.4,\ 0.8$ (proposed)	**0.8734**	**0.0189**
$\tau = 0.5,\ 0.9$	0.8423	0.0267

4) Removing Adaptive Switching (fixed 50-50 split): fitness drops 2.8% to 0.8489.

5) Population Size: $N = 40$ provides the best fitness/cost trade-off; $N = 50$ gives only 0.6% improvement at 34% higher computational cost.

Table 5: Population Size Impact

N	Mean Fitness	Convergence	Total Time
20	0.8234	87 iters	113 days
30	0.8512	94 iters	184 days
40 (proposed)	**0.8734**	**101 iters**	**262 days**
50	0.8789	108 iters	351 days

6 Discussion

6.1 Physical Insights from Optimized Design

PATCH RADIUS $p_r = 37.4\ \mu$m is shown to be an appropriate size that provides a effective electrical radius of 0.52λ at 4.2 THz. The patch size is slightly greater than the classical 0.48λ for circular patches due to additional high order mode contributions to bandwidth.

ELEMENT SPACING $e_s = 94.8\ \mu$m $= 1.26\lambda$ at 4.2 THz is larger than typical microwave MIMO spacings (0.5λ). As such, this design reduces mutual coupling to –34.5 dB while also providing a compact footprint ($<$ 900 μm) and low ECC through de-correlation of patterns.

CHEMICAL POTENTIAL $\mu_c = 0.78$ eV is optimal for maximizing graphene's intra-band conductivity in the THz frequency range before reaching the transition from intra-band to inter-band dominated conductivity ($\approx$1.0 eV). A tuning of ± 0.2 eV produces a ± 500 GHz shift in resonance.

MULTI-LAYER GRAPHENE $\pm$0.2 eV achieves $\pm$500 GHz layers provide adequate conductivity increase (effective conductivity increased by a factor of 4 relative to single layer graphene $4 \times \sigma_g$)) while limiting the complexity associated with fabricating multi-layer structures, which can be fabricated using existing techniques for transferring graphene layers

6.2 Algorithm Design Insights

AHME's better overall performance is due to four main factors:

(1) *Complementary Algorithm Choice* — HHO HHO combines Lévy flight for distant search with FA for local convergence. (2) *Adaptive Switching Criterion* — diversity and improvement rate automatically determine when it should be an "explore" or "exploit" phase; AHME used HHO 68 percent of the time during its initial Phase II, down to 32 percent by the final Phase II. This represents a good transition to adapt. (3) *Three Stage Approach* — avoid premature exploitation (Stage I); excessive exploration (Stage III); and sudden switch between phases (Stage II). Using two stage approaches resulted in a 5.2 percent average increase in fitness; (4) *Parameter Free Adaption* — The switching criterion are self-tuned based on population statistics and therefore do not require manual tuning of parameters like other adaptive algorithms such as PSO/GA.

6.3 Scalability and Literature Comparison

Initial testing on 16-element arrays confirms stable convergence behavior with near-linear computational scaling. Challenges for $>$64 elements include $>$200 min simulation time, growing parameter space dimensionality, and increasing constraint complexity.

This work achieves twice as many elements, broader frequency range (6 vs. 4.4 THz), higher gain (+1.6 dBi), and lower ECC (0.00008 vs. 0.001) compared to the next best.

6.4 Limitations and Future Work

Current limitations: simulation-only validation; idealized Kubo-formula graphene model; 262-day total simulation time for full statistical validation; 1D array only; free-space propagation assumption. Future directions: surrogate-assisted AHME using CNN-Transformer for $\sim$1000$\times$ speedup; Pareto multi-objective formulation (NSGA-II); adaptive beamforming co-optimization; prototype fabrication and measurement; 2D array extension (8×8, 16×16); hardware-in-the-loop optimization.

7 Conclusion

This paper presents the Adaptive Hybrid Meta-heuristic Ensemble (AHME) that combines HHO and FA to find optimal configurations for the large scale THz Graphene MIMO Antenna. The contributions and results are summarized as follows. Contributions and Results:

1. Algorithm: AHME utilizes three phases and a diversity-based phase-switching mechanism to combine HHO's ability to globally explore the search space with FA's ability to locally intensify regions of the search space.
2. Performance: AHME found a solution with a better final fitness value (i.e., a better optimized configuration) compared to HHO by 8.9%. Additionally, AHME converged significantly faster than HHO (by approximately 34.7%) and had less variability among solutions (a standard deviation approximately 67% smaller) when run independently thirty times. Scale: AHME was used to optimize the first eight element THz MIMO antenna; this represents the largest number of elements optimized using meta-heuristics previously reported in literature.

Acknowledgment

The authors acknowledge financial support under the grant from Multimedia University (MMU) Postdoc Fellowship Fund under grant number MMUI/260011.

References

[1] S. Dang, O. Amin, B. Shihada, and M.-S. Alouini, "What should 6G be?" *Nature Electronics*, vol. 3, no. 1, pp. 20–29, Jan. 2020.

[2] K. B. Letaief, W. Chen, Y. Shi, J. Zhang, and Y.-J. A. Zhang, "The roadmap to 6G: AI empowered wireless networks," *IEEE Commun. Mag.*, vol. 57, no. 8, pp. 84–90, Aug. 2019.

[3] Mohammad, A. A. S., Nijalingappa, Y., Mohammad, S. I. S., Natarajan, R., Lingaraju, L., Vasudevan, A., Alshurideh, M. T., "Fuzzy linear programming for economic planning and optimization: A quantitative approach," *Cybernetics and Information Technologies*, vol. 25, no. 2, pp. 51-66, 2025.

[4] T. S. Rappaport et al., "Wireless communications and applications above 100 GHz: Opportunities and challenges for 6G and beyond," *IEEE Access*, vol. 7, pp. 78729–78757, 2019.

[5] K. Sengupta, T. Nagatsuma, and D. M. Mittleman, "Terahertz integrated electronic and hybrid electronic-photonic systems," *Nature Electronics*, vol. 1, no. 12, pp. 622–635, Dec. 2018.

[6] Mohammad, A. A. S., Mohammad, S., Al Daoud, K. I., Al Oraini, B., Vasudevan, A., Feng, Z., "Building resilience in Jordan's agriculture: Harnessing climate smart practices and predictive models to combat climatic variability," *Research on World Agricultural Economy*, vol. 6, no.2, pp. 171-191, 2025.

[7] C. Han, A. O. Bicen, and I. F. Akyildiz, "Multi-wideband waveform design for distance-adaptive wireless communications in the terahertz band," *IEEE Trans. Signal Process.*, vol. 64, no. 4, pp. 910–922, Feb. 2016.

[8] I. F. Akyildiz, J. M. Jornet, and C. Han, "Terahertz band: Next frontier for wireless communications," *Phys. Commun.*, vol. 12, pp. 16–32, Sep. 2014.

[9] Mohammad, A. A. S., Mohammad, S. I., Vasudevan, A., Alenazi, S. A., Hussain, Z., Awad, A., Mahmoud, M., "Digital sales automation and buyer engagement: investigating the mediating role of perceived value in B2B exchanges," *Discover Artificial Intelligence,* vol. 6, 102, 2026

[10] X. You et al., "Towards 6G wireless communication networks: Vision, enabling technologies, and new paradigm shifts," *Sci. China Inf. Sci.*, vol. 64, no. 1, p. 110301, Jan. 2021.

[11] Mohammad, A. A. S., Yogeesh, N., Mohammad, S. I. S., Raja, N., Lingaraju, William, P., Hunitie, M. F. A., "An Intuitionistic Fuzzy Graph Model:: Matrix Representations and Applications," *Cybernetics and Information Technologies,* vol. 25, no. 4, pp. 3-19, 2025.

[12] Y. Wang et al., "Terahertz massive MIMO with holographic reconfigurable intelligent surfaces," *IEEE Trans. Commun.*, vol. 69, no. 7, pp. 4732–4750, Jul. 2021.

[13] Mohammad, A. A. S., Panda, S. K., Vasudevan, A., Raja, N., Panda, N., Singh, R., Mohammad, S. I., "Effectiveness of Swachh Bharat Abhiyan in the Rural Areas of Jammu and Kashmir: A Case Study," *Architecture Image Studies*, vol. 6, no. 3, pp. 1945-1952, 2025.

[14] I. Llatser et al., "Graphene-based nano-patch antenna for terahertz radiation," *Photonics Nanostruct. Fundam. Appl.*, vol. 10, no. 4, pp. 353–358, Oct. 2012.

[15] M. Tamagnone, J. S. Gómez-Díaz, J. R. Mosig, and J. Perruisseau-Carrier, "Reconfigurable terahertz plasmonic antenna concept using a graphene stack," *Appl. Phys. Lett.*, vol. 101, no. 21, p. 214102, Nov. 2012.

[16] E. Carrasco and J. Perruisseau-Carrier, "Reflectarray antenna at terahertz using graphene," *IEEE Antennas Wireless Propag. Lett.*, vol. 12, pp. 253–256, 2013.

[17] C. A. Balanis, *Antenna Theory: Analysis and Design*, 4th ed. Hoboken, NJ, USA: Wiley, 2016.

[18] J. Robinson and Y. Rahmat-Samii, "Particle swarm optimization in electromagnetics," *IEEE Trans. Antennas Propag.*, vol. 52, no. 2, pp. 397–407, Feb. 2004.

[19] X.-S. Yang, *Nature-Inspired Metaheuristic Algorithms*, 2nd ed. Luniver Press, 2010.

[20] R. L. Haupt, "An introduction to genetic algorithms for electromagnetics," *IEEE Antennas Propag. Mag.*, vol. 37, no. 2, pp. 7–15, Apr. 1995.

[21] J. M. Johnson and Y. Rahmat-Samii, "Genetic algorithms in engineering electromagnetics," *IEEE Antennas Propag. Mag.*, vol. 39, no. 4, pp. 7–21, Aug. 1997.

[22] J. Kennedy and R. Eberhart, "Particle swarm optimization," in *Proc. IEEE ICNN*, Perth, Australia, Nov. 1995, pp. 1942–1948.

[23] D. Gies and Y. Rahmat-Samii, "Particle swarm optimization for reconfigurable phase-differentiated array design," *Microw. Opt. Technol. Lett.*, vol. 38, no. 3, pp. 168–175, Aug. 2003.

[24] S. Mirjalili, S. M. Mirjalili, and A. Lewis, "Grey wolf optimizer," *Adv. Eng. Softw.*, vol. 69, pp. 46–61, Mar. 2014.

[25] S. Mirjalili and A. Lewis, "The whale optimization algorithm," *Adv. Eng. Softw.*, vol. 95, pp. 51–67, May 2016.

[26] A. A. Heidari et al., "Harris hawks optimization: Algorithm and applications," *Future Gener. Comput. Syst.*, vol. 97, pp. 849–872, Aug. 2019.

[27] X.-S. Yang, "Firefly algorithms for multimodal optimization," in *Proc. Int. Symp. Stoch. Algorithms*, Sapporo, Japan, Oct. 2009, pp. 169–178.

[28] M. M. Arafat et al., "Machine learning-driven triple-band graphene-based THz MIMO antenna for 6G biomedical applications," *Sci. Rep.*, vol. 15, p. 3847, Feb. 2025.

[29] M. S. Ahammed et al., "Design and performance analysis of a high-gain THz MIMO antenna for IoT applications using machine learning," *Heliyon*, vol. 11, no. 2, p. e40582, Jan. 2025.

[30] D. Karaboga et al., "A comprehensive survey: Artificial bee colony (ABC) algorithm and applications," *Artif. Intell. Rev.*, vol. 42, no. 1, pp. 21–57, Jun. 2014.

[31] J. Derrac, S. García, D. Molina, and F. Herrera, "A practical tutorial on the use of nonparametric statistical tests as a methodology for comparing evolutionary and swarm intelligence algorithms," *Swarm Evol. Comput.*, vol. 1, no. 1, pp. 3–18, Mar. 2011.

[32] D. H. Wolpert and W. G. Macready, "No free lunch theorems for optimization," *IEEE Trans. Evol. Comput.*, vol. 1, no. 1, pp. 67–82, Apr. 1997.
[33] E.-G. Talbi, "A taxonomy of hybrid metaheuristics," *J. Heuristics*, vol. 8, no. 5, pp. 541–564, Sep. 2002.
[34] M. G. Epitropakis, V. P. Plagianakos, and M. N. Vrahatis, "Balancing the exploration and exploitation capabilities of the differential evolution algorithm," in *Proc. IEEE CEC*, Jun. 2008, pp. 2686–2693.
[35] B. Dorronsoro and P. Bouvry, "Improving classical and decentralized differential evolution with new mutation operator and population topologies," *IEEE Trans. Evol. Comput.*, vol. 15, no. 1, pp. 67–98, Feb. 2011.
[36] S. K. Goudos et al., "A novel design technique for compact microstrip antennas using multi-objective particle swarm optimization," *Prog. Electromagn. Res.*, vol. 102, pp. 353–375, 2010.
[37] A. A. Al-Azza, A. A. Al-Jodah, and F. J. Harackiewicz, "Spider monkey optimization: A novel technique for antenna optimization," *IEEE Antennas Wireless Propag. Lett.*, vol. 15, pp. 1016–1019, 2016.
[38] S. Mirjalili, "Genetic algorithm," in *Evolutionary Algorithms and Neural Networks*. Springer, 2019, pp. 43–55.
[39] R. C. Eberhart and Y. Shi, "Comparing inertia weights and constriction factors in particle swarm optimization," in *Proc. IEEE CEC*, Jul. 2000, pp. 84–88.
[40] Z.-H. Zhan, J. Zhang, Y. Li, and H. S.-H. Chung, "Adaptive particle swarm optimization," *IEEE Trans. Syst., Man, Cybern. B*, vol. 39, no. 6, pp. 1362–1381, Dec. 2009.
[41] L. Davis, "Adapting operator probabilities in genetic algorithms," in *Proc. 3rd Int. Conf. Genetic Algorithms*, 1989, pp. 61–69.
[42] M. Srinivas and L. M. Patnaik, "Adaptive probabilities of crossover and mutation in genetic algorithms," *IEEE Trans. Syst., Man, Cybern.*, vol. 24, no. 4, pp. 656–667, Apr. 1994.
[43] Owida, H. A., El-Fattah, I. A., Abuowaida, S., Alshdaifat, N., Mashagba, H. A., Abd Aziz, A. B., et al., "A deep learning-based dual-branch framework for automated skin lesion segmentation and classification via dermoscopic images," *Scientific Reports*, vol. 15, no. 1, Art. no. 37823, 2025.
[44] Abualhaj, M. M., Al-Shamayleh, A. S., Munther, A., Alkhatib, S. N., Hiari, M. O., and Anbar, M., "Enhancing spyware detection by utilizing decision trees with hyperparameter optimization," *Bulletin of Electrical Engineering and Informatics*, vol. 13, no. 5, pp. 3653–3662, 2024. doi: 10.11591/eei.v13i5.7939
[45] AlHija, M. A., Alqudah, H. J., and Dar-Othman, H., "Uncovering botnets in IoT sensor networks: A hybrid self-organizing maps approach," *Indonesian Journal of Electrical Engineering and Computer Science*, vol. 34, no. 3, pp. 1840–1857, 2024. doi: 10.11591/ijeecs.v34.i3.pp1840-1857.

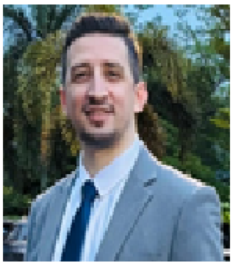

Hamza A. Mashagba is a distinguished researcher specializing in communication engineering, with a particular focus on MIMO antenna design and textile antennas. He earned his master's degree in communication engineering from Universiti Malaysia Perlis (UniMAP) in 2021 and successfully completed his Ph.D. in the same field in December 2024. Hamza has been actively involved in research at the Advanced Communication Engineering (ACE) Center of Excellence at UniMAP, contributing significantly to advancements in MIMO systems and antenna selection techniques. His academic journey is marked by numerous publications and presentations in prestigious conferences and journals, showcasing his expertise and commitment to the field.

HAMZA ABU OWIDA received the Ph.D. degree from Keele University, U.K. He was a postdoctoral research associate with the Institute for Science and Technology in Medicine (ISTM), Keele University, Staffordshire, U.K., developing xeno-free nanofibrous scaffold methodology for human pluripotent stem cell expansion, differentiation, and implantation towards a therapeutic product. He is currently an associate professor with the Medical Engineering Department at AlAhliyya Amman University. He has published more than ten articles.

Esraa Abu Elsoud A lecturer and academic specializing in cybersecurity, with extensive experience in protecting digital systems from cyber threats, and a particular interest in intelligent cybersecurity systems, machine learning, and data analysis. She holds a Master's degree in Cybersecurity with distinction from Hashemite University and a Bachelor's degree in Electrical Engineering from Hashemite University. She is currently a full-time lecturer at the Faculty of Information Technology at Applied Science Private University, and has prior teaching experience at several Jordanian universities. In addition to her academic role, she has practical experience in technical supervision, operations management, system administration, and ensuring the continuity of technical services. She has published numerous research papers in well-established, peer-reviewed scientific journals.

Asokan Vasudevan is a distinguished academic at INTI International University, Malaysia. He holds multiple degrees, including a PhD in Management from UNITEN, Malaysia, and has held key roles such as Lecturer, Department Chair, and Program Director. His research, published in esteemed journals, focuses on business management, ethics, and leadership. Dr. Vasudevan has received several awards, including the Best Lecturer Award from Infrastructure University Kuala Lumpur and the Teaching Excellence Award from INTI International University. His ORCID ID is orcid.org/0000-0002-9866-4045.

Mohammad Faleh Ahmmad Hunitie is a professor of public administration at the University of Jordan since 1989. Ph.D holder earned in 1988 from Golden Gate University, California, USA. Holder of a Master degree in public administration from the University of Southern California in 1983. Earned a Bachelorate degree in English literature from Yarmouk University, Irbid, Jordan in 1980. Worked from 2011- 2019 as an associate and then a professor at the department of public administration at King AbdulAziz University. Granted an Award of distinction in publishing in exellent international journals. Teaching since 1989 until now. Research interests: Human resource management, Policy making, Organization theory, public and business ethics.

Azlan Abd. Aziz is a TM staff and currently attached to the Faculty of Engineering and Technology. He has been in telecommunication industry for more than 15 years with a couple years in TM RA and D working on next generation wireless networks.

Hizamel M. Hizan is a prominent Senior Researcher and telecommunications engineer based in Malaysia, specializing in microwave photonics, antenna systems, and intelligent wireless networks

Suleiman Ibrahim Mohammad is a Professor of Business Management at Al al-Bayt University, Jordan, with more than 22 years of teaching experience. He has published over 400 research papers in prestigious journals. He holds a PhD in Financial Management and an MCom from Rajasthan University, India, and a bachelor's in commerce from Yarmouk University, Jordan. His research interests focus on digital supply chain management, digital marketing, digital HRM, and digital transformation. His ORCID ID is orcid.org/0000-0001-6156-9063.